




MCAM⁺ brain endothelial cells contribute to neuroinflammation by recruiting pathogenic CD4⁺ T lymphocytes

Marc Charabati,^{1,2} Stephanie Zandee,^{1,2} Antoine P. Fournier,^{1,2} Olivier Tastet,¹ Karine Thai,^{1,2} Roxaneh Zaminpeyma,¹ Marc-André Lécuyer,^{1,3} Lyne Bourbonnière,¹ Sandra Larouche,¹ Wendy Klement,¹ Camille Grasmuck,^{1,2}  Fiona Tea,^{1,2} Bettina Zierfuss,^{1,2} Ali Filali-Mouhim,¹ Robert Moumdjian,^{4,5} Alain Bouthillier,^{4,5} Romain Cayrol,^{6,7} Evelyn Peelen,^{1,2} Nathalie Arbour,^{1,2} Catherine Larochelle^{1,2,8} and Alexandre Prat^{1,2,8}

See Schneider-Hohendorf and Wiendl (<https://doi.org/10.1093/brain/awad079>) for a scientific commentary on this article.

The trafficking of autoreactive leucocytes across the blood–brain barrier endothelium is a hallmark of multiple sclerosis pathogenesis. Although the blood–brain barrier endothelium represents one of the main CNS borders to interact with the infiltrating leucocytes, its exact contribution to neuroinflammation remains understudied. Here, we show that *Mcam* identifies inflammatory brain endothelial cells with pro-migratory transcriptomic signature during experimental autoimmune encephalomyelitis. In addition, MCAM was preferentially upregulated on blood–brain barrier endothelial cells in multiple sclerosis lesions *in situ* and at experimental autoimmune encephalomyelitis disease onset by molecular MRI. *In vitro* and *in vivo*, we demonstrate that MCAM on blood–brain barrier endothelial cells contributes to experimental autoimmune encephalomyelitis development by promoting the cellular trafficking of T_H1 and T_H17 lymphocytes across the blood–brain barrier. Last, we showcase ST14 as an immune ligand to brain endothelial MCAM, enriched on CD4⁺ T lymphocytes that cross the blood–brain barrier *in vitro*, *in vivo* and in multiple sclerosis lesions as detected by flow cytometry on rapid autopsy derived brain tissue from multiple sclerosis patients. Collectively, our findings reveal that MCAM is at the centre of a pathological pathway used by brain endothelial cells to recruit pathogenic CD4⁺ T lymphocyte from circulation early during neuroinflammation. The therapeutic targeting of this mechanism is a promising avenue to treat multiple sclerosis.

- 1 Neuroimmunology Research Laboratory, Centre de Recherche du Centre Hospitalier de l'Université de Montréal (CRCHUM), Montreal, Quebec H2X 0A9, Canada
- 2 Department of Neurosciences, Université de Montréal, Montreal, Quebec H3T 1J4, Canada
- 3 Department of Microbiology, Infectious Diseases and Immunology, Université de Montréal, Montreal, Quebec H3T 1J4, Canada
- 4 Division of Neurosurgery, Centre Hospitalier de l'Université de Montréal (CHUM), Montreal, Quebec H2X 0C1, Canada
- 5 Department of Surgery, Université de Montréal, Montreal, Quebec H3C 3J7, Canada
- 6 Clinical Department of Laboratory Medicine, CHUM, Montreal, Quebec H2X 0C1, Canada
- 7 Department of Pathology and Cell Biology, Université de Montréal, Montreal, Quebec H3T 1J4, Canada
- 8 Multiple Sclerosis Clinic, Division of Neurology, CHUM, Montreal, Quebec H2L 4M1, Canada

Received March 15, 2022. Revised September 12, 2022. Accepted October 01, 2022. Advance access publication November 2, 2022

© The Author(s) 2022. Published by Oxford University Press on behalf of the Guarantors of Brain.

This is an Open Access article distributed under the terms of the Creative Commons Attribution-NonCommercial License (<https://creativecommons.org/licenses/by-nc/4.0/>), which permits non-commercial re-use, distribution, and reproduction in any medium, provided the original work is properly cited. For commercial re-use, please contact journals.permissions@oup.com

Correspondence to: Alexandre Prat
 Neuroimmunology Research Laboratory
 Centre de Recherche du Centre Hospitalier de l'Université
 de Montréal (CRCHUM), Montreal, Quebec H2X 0A9, Canada
 E-mail: a.prat@umontreal.ca

Keywords: MCAM; blood–brain barrier; BBB endothelial cells; CNS infiltration; experimental autoimmune encephalomyelitis; multiple sclerosis

Introduction

Generally diagnosed in young adults, multiple sclerosis is a debilitating neurological disorder with immense impact on quality of life. It is thought to be driven by the trafficking of autoreactive leucocytes into the CNS where they result in the formation of lesions, the pathological hallmark of multiple sclerosis. These are sporadic multifocal areas of perivascular inflammation, demyelination, axonal loss and reactive gliosis and, depending on their location, are associated with diverse symptoms of sensory, motor and cognitive disability.^{1,2} The factors responsible for the anatomical dissemination and localization of multiple sclerosis lesions across the CNS are poorly understood.

While there are several routes to infiltrate the CNS, immune cell migration across the blood–brain barrier (BBB) is a central component of multiple sclerosis pathogenesis. Structurally, the BBB interface is restricted to CNS microvessels and is composed of tightly connected endothelial cells (ECs) exposed to circulation and supported on their abluminal side by pericytes and astrocytic endfeet. Under homeostasis, the BBB protects and supports the CNS by controlling the passage of nutrients, waste and immune cells between the parenchyma and the peripheral blood.³ In multiple sclerosis, the BBB is dysregulated. Its junctional integrity is disturbed and it becomes permeable to circulating macromolecules.^{2,4,5} In the clinic, CNS vascular breakdown is routinely evaluated by gadolinium-enhanced MRI and is used as a measure of multiple sclerosis inflammatory disease activity.^{6,7} Strikingly, however, the leakiness of the BBB in multiple sclerosis lesions was shown to be unrelated to perivascular leucocyte infiltration,^{8,9} suggesting that the latter is a distinct pathological mechanism in need of further investigation.

To cross the BBB, immune cells use cell trafficking molecules that include chemokines, chemokine receptors, integrins and cell adhesion molecules.^{3,10} On contact with the BBB ECs, these molecules trigger and mediate a cascade of molecular and cellular events that eventually leads to diapedesis across the vascular wall.¹¹ In multiple sclerosis, we and others have demonstrated that pathogenic immune cell subsets, such as IFN γ - and IL-17-producing CD4⁺ T_{helper} lymphocytes (T_H1 and T_H17, respectively), infiltrate the CNS by using cell trafficking molecules that are specifically upregulated on their cell surface, such as MCAM, ALCAM and DICAM.^{12–16} Whether the BBB is actively involved in this process remains ambiguous. Since pharmaceutically blocking cell trafficking molecules was proven by the multiple sclerosis therapy natalizumab to be an effective approach to treat multiple sclerosis, deciphering novel mechanisms that grant pathogenic leucocytes access to the CNS could lead to the establishment of next-generation anti-cell-trafficking multiple sclerosis therapies.

The goal of this study was to thoroughly investigate the expression and function of MCAM on BBB ECs in autoimmune neuroinflammation. MCAM is a highly conserved 113 kDa cell surface protein that belongs to the immunoglobulin superfamily.¹⁷ Under

physiological conditions, it can be detected in relatively low levels in diverse cell types such as epithelial cells, ECs, lymphocytes and others.¹⁸ The expression of MCAM, however, was found to be highly upregulated in some cell types during development, tumorigenesis and inflammation.^{12,17–19} In this study, we demonstrate that *Mcam* expression identifies neuroinflammation-sensitive brain venous ECs with a pro-cell trafficking gene signature. In the brain of people with multiple sclerosis, MCAM expression on BBB ECs was strikingly upregulated in lesions with active inflammation. In experimental autoimmune encephalomyelitis (EAE), molecular MRI (mMRI) revealed that the presence of MCAM on the luminal surface of brain vasculature was greatest at disease onset. Last, we demonstrate that MCAM on BBB ECs contributes to autoimmune neuroinflammation by recruiting pathogenic CD4⁺ T lymphocytes, and identify ST14 as a novel ligand involved in their migration across MCAM⁺ BBB ECs.

Materials and methods

Transcriptomic analyses

The bulk RNA sequencing findings were obtained through analysis of published and publicly available datasets featuring mouse ECs from the peripheral organs and brain of control mice and mice with active EAE at different disease stages.²⁰ The single-cell RNA sequencing results were determined by analysing the transcriptomes of brain ECs and brain-infiltrating leucocytes from naïve mice and mice with active EAE at peak of disease.²¹ Differential gene expression analysis was performed using the FindMarkers function from Seurat (R package, v.4.0.1) and was relative between the compared conditions or to remaining cells within the condition. The Gene Set Enrichment Analysis (GSEA) was achieved using the Gene Ontology Molecular Function and Biological Processes databases, obtained through mSigDb's collections (<http://www.gsea-msigdb.org/gsea/msigdb/genesets.jsp?collection=GO:MF>). All other analyses were performed as per routine procedures.

Human brain tissue

Brain biopsies and autopsies were surgically collected from donors after obtaining informed consent and ethical approval (CRCHUM research ethic committee approval number BH07.001, 20.332). Multiple sclerosis samples were isolated from patients diagnosed with multiple sclerosis according to the revised 2017 McDonald's criteria.²² Multiple sclerosis lesions were histologically classified using Luxol fast blue (LFB)/haematoxylin and eosin (H&E) staining and Oil Red O staining as previously published.^{1,23} For the immunofluorescence experiments, we used frozen samples from five patients with multiple sclerosis [55- and 60-year-old females with secondary progressive multiple sclerosis (SPMS); 48- and 65-year-old males with SPMS; a 55-year-old male with primary progressive multiple sclerosis]. For rapid autopsy experiment, the

samples were obtained from two patients with multiple sclerosis (44-year-old female with relapsing-remitting multiple sclerosis and 61-year-old male with SPMS).

MCAM knockout mice

The MCAM knockout (KO) murine colony was generated in the CRCHUM animal facility on the C57BL/6 background using cryopreserved C57BL/6N-A^{tm1Brd} *Mcam*^{tm.1^(KOMP)Wtsi}/*MbpMmucd* spermatozoa purchased from the Knockout Mouse Project (KOMP). Breeding and genotyping were routinely performed as per standard protocols. Only 8–12-week-old MCAM KO homozygotes and wild-type (WT) control littermates were used for experiments.

Experimental autoimmune encephalomyelitis

All EAE experiments were approved by the Animal Care Committee of the CRCHUM in accordance with the guidelines of the Canadian Council on Animal Care (approval number N19036APs). Active EAE experiments were conducted via immunization of 8–12-week-old female C57BL/6 mice with MOG₃₅₋₅₅ (Alpha Diagnostic), as previously published^{12,16,19,24} but with one 400-ng intraperitoneal injection of pertussis toxin (List Labs) on Day 2. Passive EAE experiments were performed as per previously described protocols^{12,15,19} with the following modifications. Active EAE was first induced via immunization with MOG₃₅₋₅₅ and one 400-ng intraperitoneal injection of pertussis toxin (List Labs) on Day 2. Splenocytes were isolated from immunized female mice on Day 8, cultured in presence of T_H1/T_H17 polarizing conditions and adoptively transferred into naïve MCAM KO or WT recipient female mice on Day 12. The recipient animals received a 200-ng intraperitoneal injection of pertussis toxin (List Labs) on Day 14.

Molecular MRI

These experiments were conducted using a previously published protocol^{25,26} but with the following minor modifications. The iron microbeads were coated with an anti-MCAM antibody (clone ME-9F1, Biolegend) and injected intravenously in mice with active EAE at different disease stages (presymptomatic, onset, peak) and in control mice (naïve, CFA + PTX-injected, MCAM KO with active EAE). MCAM luminal presence was assessed by quantifying the number of signal void per brain.

Cell isolation and culture

Murine brain ECs were isolated from naïve female mice and female mice with active EAE using the adult brain dissociation kit (Miltenyi Biotec) followed by mouse CD31 Microbeads (Miltenyi Biotec), as per the manufacturer's protocols. Murine BBB ECs were isolated from naïve MCAM KO or WT mice and grown in primary cultures as previously described.¹⁵ Murine CNS-infiltrating leucocytes were isolated from MCAM KO or WT mice with passive EAE as previously published,^{16,24} or from mice with active EAE using the adult brain dissociation kit (Miltenyi Biotec) as per the manufacturer's protocol.

Murine CD4⁺ T lymphocytes were isolated from the spleen using MACS kits (Miltenyi Biotec), and then activated and polarized *in vitro* into T_H1 and T_H17, as previously published^{16,27} but with the following modifications. *In vitro* activation of CD4⁺ T lymphocytes was achieved by incubation of cells on 10 µg/ml plate-bound anti-CD3 (clone 145-2C11, Bio X Cell) in presence of 2 µg/ml anti-CD28 (clone

37.51, BD Biosciences). *In vitro* polarized T_H1 lymphocytes were generated by adding 10 ng/ml recombinant mouse IL-12 (R&D Systems) and 20 µg/ml anti-IL-4 (clone 11B11, Bio X Cell) to the culture media during CD4⁺ T lymphocyte activation. *In vitro* polarized T_H17 lymphocytes were generated with the addition of 20 ng/ml recombinant mouse IL-6 (R&D Systems), 20 ng/ml recombinant mouse IL-23 (R&D Systems), 4 ng/ml recombinant human (rh) TGFβ (R&D Systems) and 20 µg/ml anti-IFNγ (clone XMG1.2, Bio X Cell).

Human BBB ECs were isolated from non-epileptic surgical specimens (resection path) and grown in primary cultures as previously described.^{19,28-30} Multiple sclerosis lesion-infiltrating leucocytes were isolated from rapid autopsy brains and processed as previously published.^{23,31}

Human peripheral blood mononuclear cells were isolated from blood samples of healthy donors as previously published,¹⁹ after obtaining informed consent in accordance with institutional guidelines [Centre Hospitalier de l'Université de Montréal (CHUM) research ethic committee approval number BH07.001, 20.332]. Human CD4⁺ T lymphocytes were isolated from the peripheral blood mononuclear cells using MACS kits (Miltenyi Biotec) as previously described.¹⁶

Immunofluorescence

For human immunohistochemistry staining, brain tissue blocks were frozen in 2-methylbutane and cryosectioned (7-µm thick). To stain, tissue sections were air dried, fixed in ice-cold acetone for 10 min and delipidized in 70% ethanol for 5 min. Endogenous avidin/biotin and non-specific antibody binding sites were blocked using an avidin-biotin blocking kit (Thermo Fisher Scientific) and 10% species-specific serum (Thermo Fisher Scientific) of the secondary antibody host, respectively. Sections were then incubated in blocking buffer containing primary antibodies overnight at 4°C. On the next day, slides were washed with 0.05% PBS-Tween-20 (Sigma-Aldrich) and mounted in Mowiol containing TO-PRO-3 (Thermo Fisher Scientific). Each experiment included negative controls (secondary antibodies only). Mouse immunohistochemistry staining was performed as previously described.¹⁶ The mouse and human immunocytochemistry stainings were also executed as we previously reported.^{12,32,33} Images (z-stacks) were acquired using a Leica SP5 confocal microscope with Leica LAS AF software and processed using Fiji, LAS X and Imaparis. All acquisition settings were kept the same within each experiment.

Flow cytometry

All flow cytometry cell processing, extracellular and intracellular staining, acquisition and analysis were conducted as previously described.^{16,19,23,31,34} We used antibodies that targeted human or mouse CD3, CD4, CD8, CD45, CD45RA, CD45RO, MCAM, ST14, VEGFR2, Galectin-3, IFNγ and IL-17 (BD Biosciences, R&D Systems, Miltenyi Biotec, Biolegend). Cell acquisition was done using a BD LSRII cytometer (BD Biosciences) or BD FORTESSA cytometer (BD Biosciences). Cell analysis was performed using BD FACSDiva software (BD Biosciences) or FlowJo software (FlowJo, LLC). Our gating strategy excluded doublets as per routine gating strategies, as well as dead cells stained with LIVE/DEAD fixable Aqua dead cell stain kit (Thermo Fisher Scientific) as per the manufacturer's instructions. Positive gates were defined using isotype controls and fluorescence minus one controls.

In vitro blood–brain barrier endothelial cell stimulation assay

Confluent primary cultures of human BBB ECs were either left untreated, cultured in presence of activated CD4⁺ T cells or treated with rh 100 U/ml IFN γ (Thermo Fisher Scientific) and rh 100 U/ml TNF α (Thermo Fisher Scientific), 100 U/ml of each alone, 1 ng/ml rh IL-1 β (R&D Systems), 100 ng/ml rh IL-17 (R&D Systems), 100 ng/ml rh GM-CSF (BD Biosciences) or 40% ACM. After an overnight incubation at 37°C, cells were washed with PBS, treated with PBS-EDTA for 5 min at 37°C, dissociated with 1 \times trypsin (Thermo Fisher Scientific) and processed for flow cytometry analysis. For the immunocytofluorescence assays, the primary cultures of human or mouse BBB ECs were directly cultured on specialized chamber slides (Ibidi) before stimulation and analysis via confocal microscopy.

Murine adhesion and migration assays

The *in vitro* murine flow adhesion assay was conducted using the Ibidi system and slides as previously described^{12,15,31} with the exception of using *in vitro* activated CD4⁺ T, polarized T_H1 or T_H17 lymphocytes. The *in vitro* murine migration assay was adapted from the previously published *in vitro* human migration assay^{14,30,31,35} by including the following modifications. Primary cultures of mouse BBB ECs were plated on Boyden chamber inserts coated with 0.5% gelatin (Sigma-Aldrich) containing 25 μ g/ml collagen IV (Sigma-Aldrich) for 30 min at room temperature. After 4 days in culture at 37°C, BBB ECs culture media in both upper and lower Boyden chamber compartments was replaced with Dulbecco's Modified Eagle Medium (Thermo Fisher Scientific) containing 20% foetal bovine serum (Thermo Fisher Scientific) and 100 U/ml penicillin-streptomycin (Thermo Fisher Scientific), and *in vitro* activated murine CD4⁺ T, polarized T_H1 or polarized T_H17 lymphocytes were added to the top compartment in triplicates. The migrated cells in the bottom compartments were collected and counted using a haemocytometer after an overnight incubation at 37°C.

Human migration assay

The *in vitro* human migration assay was conducted as previously described^{14,30,31,35} with the following modifications. Before the addition of peripheral blood mononuclear cells to the top compartment of the Boyden chamber, the primary cultures of human BBB ECs plated on the inserts were first stimulated for 18 h at 37°C with 100 U/ml rh IFN γ and 100 U/ml rh TNF α (both from Thermo Fisher Scientific), and then treated for 1 h at 37°C with 40 μ g/ml MCAM blocking monoclonal antibody (clone P1H12) or equivalent amount of its isotype control (both from BD Biosciences) and washed with warm media. After an overnight incubation at 37°C, the migrated cells in the bottom compartments were collected, counted using a haemocytometer and analysed via flow cytometry.

Data availability

The data that support the findings of this study are available from the corresponding author, on reasonable request.

Results

MCAM identifies capillary-to-venous brain ECs with a cell trafficking gene signature in EAE

We have previously shown that MCAM is expressed on BBB ECs.¹² To determine the physiological and pathological relevance of this expression, we explored publicly available bulk RNA sequencing datasets of ECs gathered from different organs in naïve mice, and from brains of mice with active MOG₃₅₋₅₅ EAE at different disease stages.²⁰ In naïve animals, the expression of *Mcam* in brain ECs was ~4–14 times lower than in ECs from liver, heart, kidney and lung in naïve animals (Fig. 1A). However, *Mcam* brain expression increased following EAE induction, particularly at the early phase of the disease: that is, when immune cells are actively infiltrating the CNS (Fig. 1B). In comparison with other cell trafficking molecules known to be involved in autoimmune neuroinflammation, the expression level and fold upregulation of *Mcam* mRNA in brain ECs at EAE disease onset were similar to those of *Icam1* and *Vcam1*, and greater than those of *Alcam* (Fig. 1C).

To comprehensively characterize the profile of *Mcam*⁺ BBB ECs, we analysed a dataset of single-cell RNA profiles of ECs isolated from the brains of naïve and MOG₃₅₋₅₅-immunized EAE animals.²¹ Compared to naïve mice, computational analyses first confirmed the increase in *Mcam* mRNA average expression in brain ECs in EAE mice and further revealed an increase in the frequency of *Mcam*⁺ brain ECs in EAE (Fig. 1D). A global comparison of *Mcam*⁺ brain ECs in EAE versus naïve animals identified 385 differentially expressed genes (DEGs), including 215 upregulated and 170 downregulated DEGs, in *Mcam*⁺ ECs in EAE, compared to naïve mice (Fig. 1E). Interestingly, the prototypical cell trafficking molecules *Vcam1* and *Icam1* were both detected among the significantly upregulated DEGs in *Mcam*⁺ ECs in EAE (Supplementary Table 1). GSEA subsequently demonstrated a statistically significant upregulation of 201 pathways and downregulation of 178 pathways *Mcam*⁺ ECs in EAE (Fig. 1F and Supplementary Table 2). Among the significantly modulated pathways, while we noted the downregulation of multiple pathways linked with angiogenesis and EC movement, the upregulation of numerous inflammatory- and immune-associated mechanisms, including immune cell trafficking, was striking, suggesting that *Mcam*⁺ brain ECs play various neuroinflammatory functions in EAE.

Having previously shown that mouse brain ECs can be transcriptionally organized on the basis of gradients of gene expression rather than distinct clustering,²¹ we next sought to further characterize the expression of *Mcam* in brain ECs along an arteriovenous axis reflective of the cerebrovascular tree. To generate this axis, we used a pseudotime analysis to unbiasedly rank the sequenced ECs along a transcriptomic trajectory and confirmed its arteriovenous architecture using previously published markers.³⁶ Examining the relative distribution density of *Mcam*⁺ ECs along this axis then revealed that, in naïve animals, *Mcam*⁺ brain ECs mostly correlated with the arterial portion of the axis (Fig. 1G). In EAE, however, we observed an upregulation in the density of *Mcam*⁺ ECs along the venous portion of the axis (Fig. 1G).

To determine a specific pathological function associated with *Mcam*⁺ brain ECs in EAE, we focused on its expression in capillary-to-venous brain ECs. Strikingly, we found only 46 DEGs (40 upregulated, six downregulated) enriched in *Mcam*⁺ capillary-to-venous ECs in naïve animals, but 123 DEGs (89 upregulated, 34 downregulated) in EAE animals (Fig. 1H), indicating that these cells are highly reactive to autoimmune neuroinflammation.

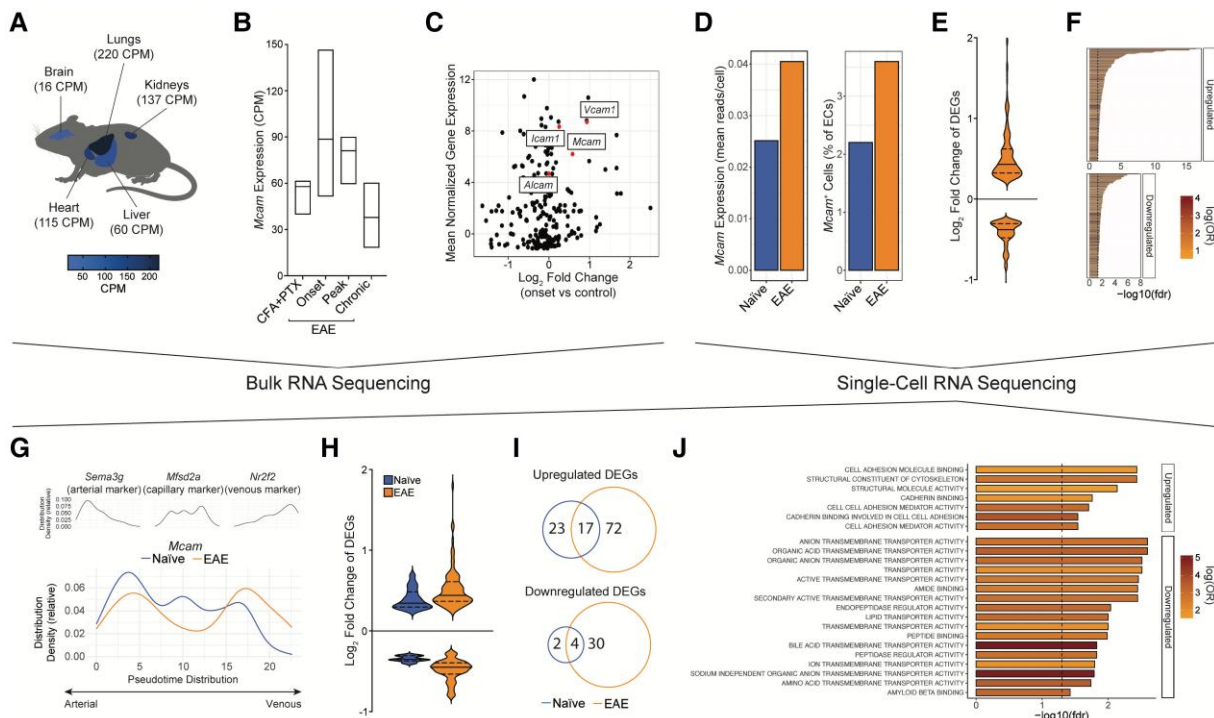


Figure 1 *Mcam* expression in brain endothelial cells correlates with onset of neuroinflammation and is associated with a pro-migration gene signature. (A–C) Analysis of bulk RNA sequencing dataset of peripheral and brain ECs.²⁰ (A) *Mcam* mRNA expression [mean counts per million (CPM)] in ECs from lung, kidney, heart, liver and brain of naïve mice, projected on anatomical mouse sketch. (B) *Mcam* mRNA expression (mean CPM, min to max) in brain ECs from control mice injected with CFA and PTX and EAE mice at different disease stage. (C) Scatter plot showing the mean normalized expression of genes of immunoglobulin subtype at EAE disease onset and their log fold change at disease onset compared to control animals. (D–J) Analysis of single-cell RNA sequencing dataset of brain ECs in naïve and EAE mice.²¹ (D) Left and right bar charts show *Mcam* mRNA expression (mean read per cell ± SEM) in ECs and frequency of *Mcam*⁺ ECs (mean of total ECs ± SEM), respectively, in brains of naïve and EAE mice. (E) Violin plot (\log_2 fold change) and (F) GSEA of the DEGs in *Mcam*⁺ ECs in EAE; $P < 0.05$. (G) Distribution density (relative to 100% of cells per condition) along the arteriovenous axis of brain ECs expressing markers of arterial, capillary and venous ECs (top), and *Mcam* in naïve and EAE mice (bottom). (H) Violin plot (\log_2 fold change) of the DEGs in *Mcam*⁺ brain capillary-to-venous ECs (relative to the remaining cells per condition). (I) Venn diagrams showing their overlap in naïve and EAE mice. (J) GSEA of the DEGs in *Mcam*⁺ brain capillary-to-venous ECs unique to EAE.

Among the DEGs associated with *Mcam* expression, 72 and 30 were exclusively upregulated and downregulated in EAE, respectively (Fig. 1I). GSEA demonstrated that the upregulated EAE-specific DEGs were mostly associated with cell adhesion pathways, whereas the downregulated DEGs were mainly linked to metabolic and transport activities (Fig. 1J). Altogether, our RNA sequencing analyses revealed that *Mcam*⁺ capillary-to-venous ECs are reactive to EAE development and feature a transcriptomic signature associated with cell trafficking.

BBB ECs upregulate MCAM expression in multiple sclerosis lesions and in presence of inflammatory stimuli

Multiple sclerosis lesions are the pathological signature of the disease; they are characterized by varying degrees of demyelination and neuroinflammation, and are classified accordingly.¹ Having previously detected MCAM on the BBB in the brain of individuals with multiple sclerosis, we sought to fully characterize its expression on the endothelium in the different types of lesions by immunofluorescent confocal microscopy. In brain tissue from five patients with multiple sclerosis, lesion types were defined using a combination of H&E/LFB, and Oil Red O stains, as per standard histological protocols.^{23,32} After identifying and localizing BBB ECs on each tissue section using CD31 or laminin $\alpha 4$ (LAMA4)

co-immunostainings, quantification of MCAM mean signal intensity revealed a 1.7- and 2.3-fold upregulation in pre-active and active multiple sclerosis lesions, respectively, as compared to in normal appearing white matter (NAWM) (Fig. 2A and B). Intriguingly, the greatest increase in MCAM signal intensity was found in normal appearing tissue adjacent to active lesions: that is, where the lesion would be expected to expand (Fig. 2A and B). In mixed active/inactive lesions, MCAM signal intensity significantly increased by 2.3-fold at the active borders but not at the inactive lesion centre. Similarly, we found a relatively weaker increase in MCAM signal intensity in inactive lesions. In comparison to MCAM, the mean signal intensity of CD31 failed to statistically correlate with specific multiple sclerosis lesion types when compared to in NAWM, but was nonetheless found to be significantly increased at the border of mixed active/inactive lesions (Fig. 2C).

The increase in MCAM signal intensity in leucocyte-lacking tissue adjacent to active lesions insinuated that MCAM expression on BBB ECs is potentially induced by infiltrating leucocytes and/or secreted inflammatory molecules. To address this hypothesis, we analysed via flow cytometry the expression of MCAM on primary cultures of human BBB ECs after coculture with activated human CD4⁺ T cells or stimulation with different inflammatory cytokines. Compared to untreated BBB ECs, quantification of mean fluorescence intensity of MCAM expression on the BBB ECs showed a statistically significant upregulation after the coculture (Supplementary Fig. 1A),

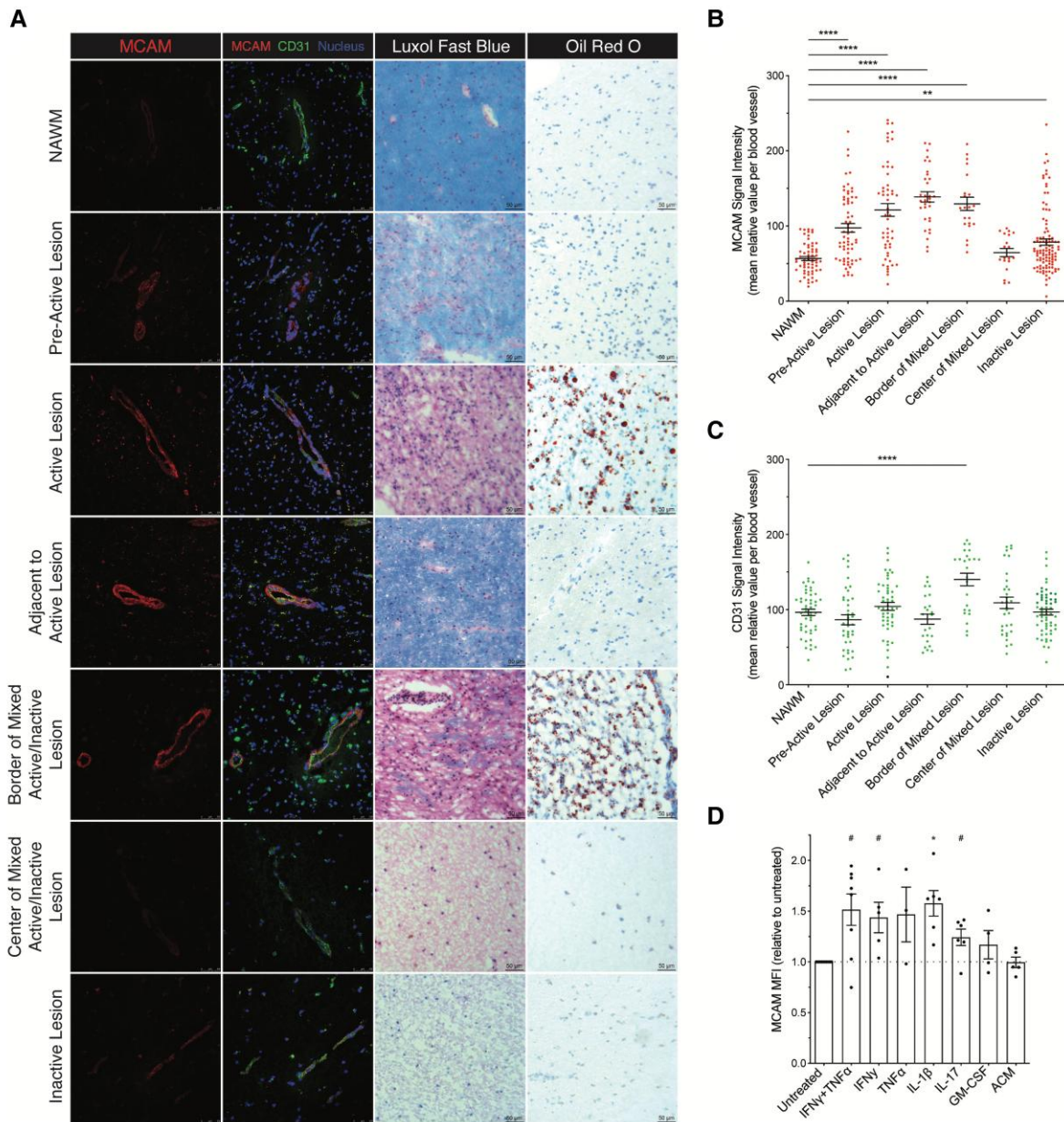


Figure 2 MCAM expression by BBB ECs is upregulated in multiple sclerosis lesions and by Inflammatory Stimuli. (A–C) Immunofluorescence analysis of MCAM expression on BBB ECs; Adjacent to Active Lesion refers to the relatively NAWM found on the same tissue section as an active lesion; $n > 5$ patients with multiple sclerosis. (A) Representative images of multiple sclerosis brain tissue sections co-stained for MCAM, CD31 and nuclei and histologically classified by LFB/H&E and Oil Red O stainings; the histological characterization was performed on consecutive tissue sections from the same frozen tissue blocks. (B and C) Unbiased quantification of the signal intensity (mean relative value \pm SEM) of (B) MCAM and (C) CD31 per cerebral blood vessel; $n \geq 18$ blood vessel per condition; P by one-way ANOVA with Dunnett's correction. (D) MCAM protein expression [mean fluorescence intensity (MFI) relative to untreated control \pm SEM] on primary *in vitro* cultures of human BBB ECs after treatment with the specified conditions; ACM refers to astrocyte-conditioned media $n \geq 3$ donors per condition; P by paired *t*-test after multiple testing correction using false discovery method; data were log transformed before statistical testing; # = 0.06.

on treatment with IL-1 β , and a borderline statistically significant up-regulation ($P = 0.06$ after multiple testing correction) on treatments with IFN γ +TNF α , IFN γ alone and IL-17 (Fig. 2C). The increase in MCAM expression on treatment with IFN γ +TNF α was subsequently confirmed to be statistically significant via immunocytofluorescence staining (Supplementary Fig. 1B and C). Treatments with TNF α alone, GM-CSF and astrocyte conditioned medium (control) had no significant effect on MCAM mean fluorescence intensity (Fig. 2C). The data generated using human biological material thus demonstrate

that the tight association of MCAM on BBB ECs with neuroinflammation is immune-associated and pathologically relevant in multiple sclerosis.

The luminal presence of MCAM on brain ECs is induced by autoimmune neuroinflammation

On the cell surface of ECs outside of the CNS, MCAM was mainly, although not exclusively, described as a junctional protein.³⁷ To

explore the cellular localization of MCAM on BBB ECs, we evaluated the pixel intensity of its immunostaining across the microvessels detected on multiple sclerosis brain tissue sections in comparison with that of CD31, which is enriched at the intercellular endothelial borders.^{38,39} In NAWM, pixel intensity of MCAM immunostaining strongly colocalized with that of CD31 (Fig. 3A), suggesting that under homeostasis, MCAM on BBB ECs is indeed predominantly junctional. In multiple sclerosis lesions, however, the molecular distribution of MCAM on BBB ECs varied according to lesion type. Strikingly, active lesions featured high MCAM pixel intensity that colocalized less with CD31 and spanned a wider segment of the microvascular walls (Fig. 3B). On the other hand, in chronic inactive lesion, the molecular distribution of MCAM and CD31 reverted to being virtually identical, similar to that in NAWM (Fig. 3C).

Since these semiquantitative observations suggested that MCAM spreads across the BBB endothelial membrane specifically during active neuroinflammation, we elected to validate this hypothesis *in vivo* via mMRI.^{25,26} Briefly, we coated iron microbeads with anti-MCAM antibody, injected them directly into the circulation of control and EAE mice, and assessed their binding to MCAM on brain vasculature by quantifying the reflected MRI-triggered signal voids (Fig. 3D). The injection of anti-MCAM microbeads in naïve mice and in control mice immunized with the adjuvants CFA and PTX without MOG₃₅₋₅₅ yielded a low number (~5) of signal voids per brain (Fig. 3E and F), implying that under homeostasis and in absence of CNS autoimmunity, MCAM on brain vasculature is rarely exposed to circulation. In mice with active MOG₃₅₋₅₅ EAE, the average number signal void per brain was similarly low during the pre-symptomatic phase but increased by ~7-fold at onset, reaching statistical significance when compared to controls, and by ~5-fold at peak of disease (Fig. 3E and F). The specificity of the detected signal voids, and thus of the anti-MCAM microbeads, were confirmed by their almost complete absence in MOG₃₅₋₅₅-immunized MCAM KO EAE mice (Fig. 3E and F). In addition, histological analysis demonstrated that the anti-MCAM microbeads exclusively colocalized with MCAM⁺ brain vessels without binding to infiltrating CD4⁺ T cells (Supplementary Fig. 2). The data presented in this section via *in situ* human and *in vivo* murine approaches thus suggest that MCAM on BBB ECs is a junctional protein that becomes exposed to the circulating peripheral blood only during active neuroinflammation.

MCAM on BBB ECs promote EAE disease development by recruiting T_H1 and T_H17 lymphocytes

IFN γ - and IL-17-producing CD4⁺ T_{helper} lymphocytes (T_H1 and T_H17, respectively) are widely considered to be among the main orchestrators of multiple sclerosis lesion formation. Their migration across the BBB is a multistep process that comprises leucocyte rolling over the endothelium, adhesion onto it and transmigration across of it.¹¹ To investigate whether MCAM on BBB ECs contributes to any of these steps, we isolated BBB ECs from whole-body MCAM KO mice or WT littermates and generated primary cultures. Flow cytometry and immunocytofluorescence analyses both confirmed that MCAM was indeed absent in the primary cultures of BBB ECs from MCAM KO but not the WT littermates (Supplementary Fig. 3). We then conducted *in vitro* flow adhesion assays to specifically assess the rolling and adhesion of *in vitro* activated CD4⁺ T lymphocytes treated with α CD3 and α CD28, and of polarized T_H1 and T_H17 cells while dynamically flowing over WT or MCAM KO BBB ECs monolayers. Since this assay involved a coculture with

activated and polarized inflammatory CD4⁺ T cells, the BBB ECs were kept unstimulated to prevent their over-stimulation, which yields abnormal adhesion and uninterpretable data. In absence of MCAM on BBB endothelium, the velocities of broadly activated CD4⁺ T, T_H1 and T_H17 lymphocytes were all significantly increased (Fig. 4A and B), thereby reflecting their significantly impaired rolling capability. However, the firm arrest under flow of T_H1 and T_H17 lymphocytes, but not of broadly activated CD4⁺ T lymphocytes, was significantly reduced on MCAM KO BBB ECs, when compared to WT BBB ECs (Fig. 4C and D). Next, we performed *in vitro* migration assays using a modified Boyden chamber system and quantified the transmigration of the same T_H lymphocyte groups across monolayers of MCAM KO versus WT BBB ECs. In line with our findings, the absence of MCAM on BBB ECs significantly reduced the transmigration of T_H1 and T_H17 lymphocytes but not that of broadly activated T_H lymphocytes (Fig. 4E–J). Our *in vitro* data hereby demonstrated that MCAM on BBB ECs specifically promotes the cell trafficking of T_H1 and T_H17 lymphocytes but not generally activated CD4⁺ T lymphocytes across the BBB.

To determine the contribution of MCAM expression by BBB ECs to autoimmune neuroinflammation, we monitored disease development in passive EAE induced by adoptively transferring WT MOG₃₅₋₅₅-specific T_H1/T_H17-polarized splenocytes into WT or MCAM KO recipients. Disease severity (up to Day 26), weight loss (up to day 19) and disease incidence were all found to be significantly reduced in MCAM KO mice as compared to in their WT littermates (Fig. 4K–M). In agreement with our previous observations, flow cytometry analysis of CNS-infiltrating leucocytes revealed a significant decrease in the global number of CD4⁺ T lymphocytes in MCAM KO mice and, more specifically, in the numbers of IFN γ ⁺ (i.e. T_H1), IL-17⁺ (i.e. T_H17) and IFN γ ⁺ IL-17⁺ (i.e. IFN γ ⁺ T_H17) CD4⁺ T lymphocytes (Fig. 4N–Q). Strikingly, these decreases were observed at disease onset but not later (Fig. 4N–Q), thereby corresponding with our mMRI data and the absence of statistically significant difference in clinical disease parameters at the later stages (clinical score and weight loss, from Days 26 and 19 onwards, respectively). Collectively, our findings show that MCAM on BBB ECs contribute to the onset of neuroinflammation by promoting the migration of pathogenic CD4⁺ T lymphocytes into the CNS.

ST14⁺ CD4⁺ T lymphocytes preferentially cross MCAM⁺ BBB ECs and accumulate during autoimmune neuroinflammation

Over the last decade, MCAM was described to interact with an increasing number of ligands. In the literature, we identified MCAM (homotypic interaction), ST14, VEGFR2 and Galectin-3 as candidate ligands that could be expressed and used by pathogenic CD4⁺ T lymphocytes to migrate across MCAM⁺ BBB ECs. To address this hypothesis, we sought to investigate the *in vitro* migration of CD4⁺ T lymphocyte across primary cultures of human BBB ECs. To specifically target MCAM on human BBB ECs without interfering with its presence and function on CD4⁺ T cells,¹² we stimulated the primary cultures of BBB ECs with IFN γ and TNF α overnight, pretreated them with MCAM blocking antibody or isotype control and washed off the excess antibodies before adding leucocytes to the Boyden chamber. Given our observations that MCAM on human BBB ECs is significantly upregulated in presence of activated CD4⁺ T cells and inflammatory cytokine, we performed this experiment using unstimulated leucocytes to prevent the upregulation of MCAM following its surface neutralization with the blocking antibody.

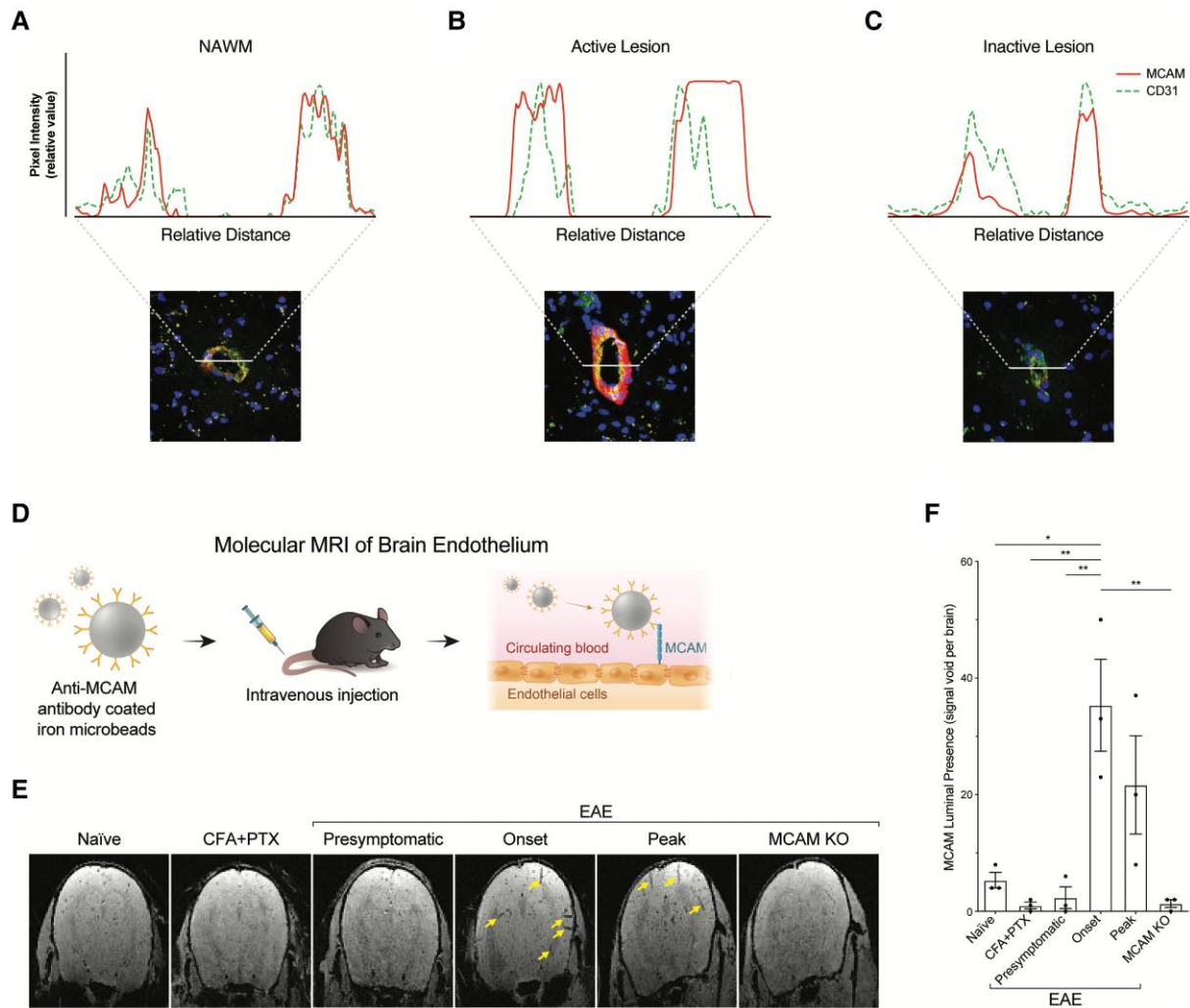


Figure 3 Autoimmune neuroinflammation triggers the luminal presence of MCAM on cerebral blood vessels. (A–C) Representative immunofluorescence analysis of the vascular localization of MCAM and CD31 in multiple sclerosis brain tissue sections co-stained for MCAM, CD31 and nuclei, and characterized histologically as (A) NAWM, (B) active lesion and (C) inactive lesion by LFB/H&E and Oil Red O stainings. (A–C) Pixel intensity of each signal was measured across lines drawn to intercept the axis of each blood vessel. (D) Schematic representation, (E) representative images and (F) quantification of the presence (mean signal void per brain \pm SEM) of MCAM on the luminal side of brain blood vessels, as measured by mMRI after injection of anti-MCAM antibody coated iron microbeads in mice with active EAE at different disease stages (presymptomatic, onset, peak) and in control mice (naïve, injected with CFA and PTX without MOG, EAE in MCAM KO); $n = 3$ mice per condition. (E) Yellow arrows indicate signal voids. (F) P by one-way ANOVA with Bonferroni correction.

Corroborating our murine findings, we first found that selectively blocking MCAM on inflamed human BBB ECs reduced the migration of CD4⁺ T lymphocytes (Fig. 5A and B). To evaluate the potential involvement of each candidate ligand in CD4⁺ T lymphocyte migration, we then measured their surface expression on migrated versus non-migrated T lymphocytes using flow cytometry and then calculated their expression frequency ratio. Under control condition (i.e. after blocking with isotype control), only the frequency ratio of MCAM⁺ and ST14⁺ CD4⁺ T lymphocytes (Fig. 5C–F) were significantly >1 (one sample *t*-test; $P = 0.0042$ and 0.0356 , respectively), thereby indicating that MCAM⁺ and ST14⁺ CD4⁺ T lymphocytes preferentially migrated across the BBB ECs. Strikingly, when MCAM on BBB ECs was blocked, both frequency ratios got significantly reduced (Fig. 5C–F) and became no longer statistically >1 (one sample *t*-test).

Since the expression and function of MCAM on CD4⁺ T lymphocytes has already been the subject of several studies by us and

others,^{12,13,40} we focused hereafter on ST14. By flow cytometry, we observed that ST14 expression on CD4⁺ T lymphocytes was significantly greater on memory CD45RO⁺ than on naïve CD45RA⁺ CD4⁺ T lymphocytes (Fig. 5G and H). To investigate whether MCAM on BBB ECs promotes the trafficking of memory CD45RO⁺ CD4⁺ T lymphocytes through ST14, we examined the effect the MCAM blocking monoclonal antibody on the migration of total and ST14⁺ memory CD45RO⁺ CD4⁺ T lymphocytes. Selectively blocking MCAM on the inflamed primary cultures of human BBB ECs was found to significantly reduce the trafficking of total and ST14⁺ memory CD45RO⁺ CD4⁺ T lymphocytes by ~20 and 40%, respectively (Fig. 5I–L), suggesting that MCAM on BBB ECs is specifically involved in recruiting ST14⁺ memory CD45RO⁺ CD4⁺ T lymphocytes during inflammation.

Last, to examine the pathological relevance of these findings, we assessed the CNS presence of ST14⁺ CD4⁺ T lymphocytes in autoimmune neuroinflammation. In EAE, single-cell RNA sequencing

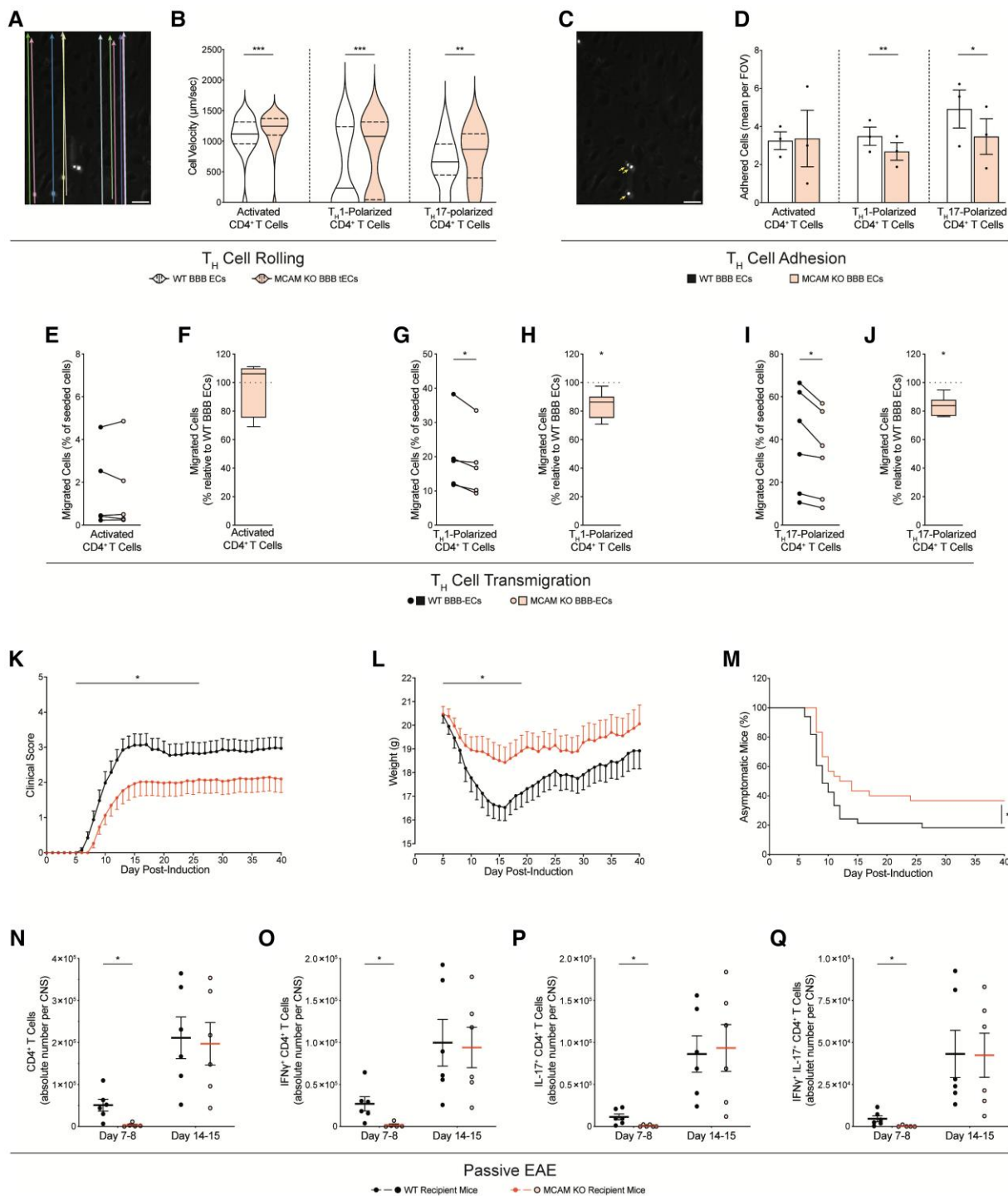


Figure 4 MCAM on the BBB promotes the trafficking of T_H1 and T_H17 lymphocytes into the CNS and the development of EAE. (A) Representative image of the automated vectors used to unbiasedly track cell velocity, (B) quantification of cell velocity (mean µm/s ± SEM), (C) representative image of adhered cells (identified with arrows) and (D) quantification of adhesion [mean absolute number of adhered cells per field of view (FOV) ± SEM], of *in vitro* activated CD4⁺ T, Th1-polarized or Th17-polarized murine lymphocytes while dynamically flowing for 20 min over primary cultures of WT or MCAM KO BBB ECs. (A–C) Representative of n = 3 independent experiments; P by Mann–Whitney test. (D) Pooled from n = 3 per group; P by paired t-test. (E–J) Migration of (E–F) *in vitro* activated CD4⁺ T, (G and H) Th1-polarized and (I and J) Th17-polarized murine T lymphocytes, across primary cultures of WT or MCAM KO BBB ECs; pooled from n = 5–6 per group. (E, G and I) Absolute proportion (mean percentage of seeded cells ± SEM); P by paired t-test. (F, H and J) Normalized proportion (median percentage, min to max, relative to WT control); P by Wilcoxon signed-rank test. (K–Q) Passive EAE in WT versus MCAM KO mice injected with *in vitro* polarized splenocytes from MOG_{35–55}-immunized WT mice. (K) Disease development (clinical score ± SEM), (L) weights (g ± SEM) and (M) disease incidence (% of asymptomatic mice), as evaluated daily; pooled from n = 4 independent experiments with a total of 33 WT and 30 MCAM KO recipient animals. (K and L) P by Mann–Whitney test on area under the curve. (M) P by log rank test. (N–Q) Quantification of CNS-infiltrating (N) total, (O) IFN γ ⁺, (P) IL-17⁺ and (Q) double positive IFN γ ⁺ IL-17⁺ CD4⁺ T lymphocytes (mean absolute number of cells per CNS ± SEM), at 7–8 and 14–15 days after EAE induction; pooled from n = 5–6 mice; P by Student’s t-test.

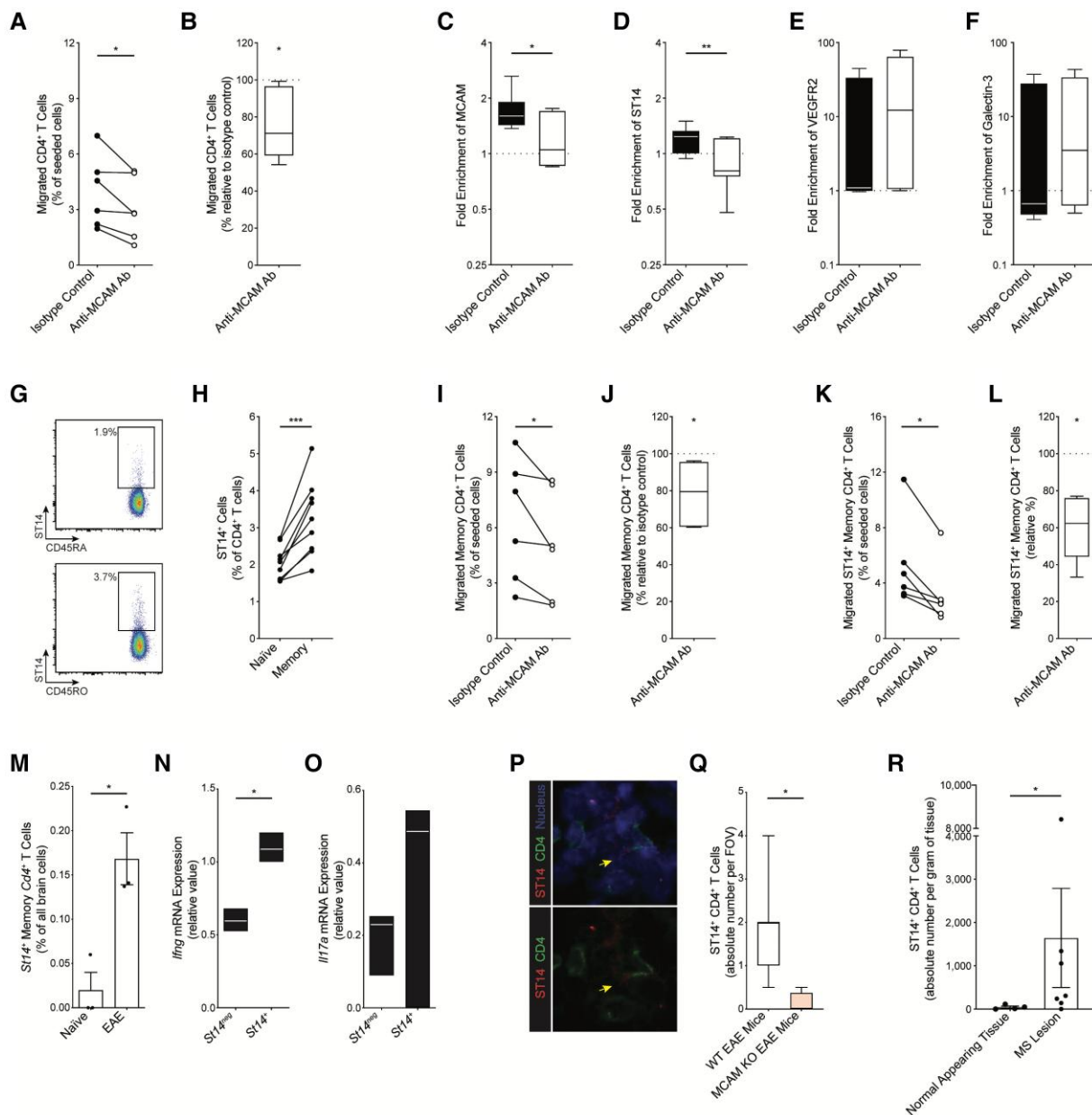


Figure 5 ST14⁺ CD4⁺ T cells preferentially migrate across inflamed MCAM⁺ BBB ECs and infiltrate the brain in EAE and multiple sclerosis. (A and B) Migration of human CD4⁺ T lymphocytes across primary cultures of human BBB ECs that were stimulated *in vitro* with IFN γ and TNF α and pretreated with isotype control or anti-MCAM antibody; $n = 6$ donors. (A) Absolute proportion (mean percentage, %, of seeded cells \pm SEM); P by paired t-test. (B) Normalized proportion (median %, min to max, relative to isotype-treated control); P by Wilcoxon signed-rank test. (C–F) Frequency ratio (mean expression ratio on migrated over non-migrated cells \pm SEM) of (C) MCAM, (D) ST14, (E) VEGFR2 and (F) Galectin-3 in human CD4⁺ T lymphocytes, as measured by flow cytometry post-migration assay. (G) Representative density plots and (H) frequency (mean \pm SEM) of ST14 protein expression on *ex vivo* naive CD45RA⁺ and memory CD45RO⁺ CD4⁺ T lymphocytes from healthy donors, as measured by flow cytometry; $n = 9$; P by paired t-test. (I–L) Migration of human (I and J) total and (K and L) ST14⁺ memory CD45RO⁺ CD4⁺ T lymphocytes across primary cultures of human BBB ECs that were stimulated *in vitro* with IFN γ and TNF α and pretreated with isotype control or anti-MCAM antibody; $n = 6$ donors. (I and K) Absolute proportion (mean % of seeded cells \pm SEM); P by paired t-test. (J and L) Normalized proportion (median %, min to max, relative to isotype-treated control); P by Wilcoxon signed-rank test. (M–O) Analysis of single-cell RNA sequencing dataset of brain cells in naive and EAE mice (Fournier et al. 2022); $n = 3$ animals per condition. (M) Frequency (mean % of brain cells \pm SEM) of St14⁺ memory Cd4⁺ T lymphocytes in naive versus EAE mice; P by Student's t-test. (N and O) Quantification (mean relative value, min to max) of *Ifng* and *Il17a* mRNA expression in St14⁺ versus St14^{neg} memory Cd4⁺ T lymphocytes in the EAE brains; P by paired t-test. (P) Representative magnified image, and (Q) absolute number [median per field of view (FOV), min to max] of brain-infiltrating ST14⁺ CD4⁺ T cells at passive EAE disease onset, as evaluated by immunohistochemistry staining of ST14, CD4 and nuclei on brain tissue sections from WT and MCAM KO recipient mice; $n = 4$; P by Student's t-test. (R) Absolute number (mean per gram of tissue \pm SEM) of ST14⁺ CD4⁺ T lymphocytes isolated from rapid autopsy multiple sclerosis normal appearing brain tissue or lesion, as measured by flow cytometry; $n = 4$ –7 tissue samples from two donors; P by Student's t-test.

analysis revealed that the frequency of brain-infiltrating St14⁺ memory Cd4⁺ T lymphocytes is significantly greater than in naive animals (Fig. 5M). When compared to St14^{neg} memory Cd4⁺ T

lymphocytes, EAE brain-infiltrating St14⁺ memory Cd4⁺ T lymphocytes expressed significantly greater levels of *Ifng* and a greater trend of *Il17a*, (Fig. 5N and O), highlighting the potential *in vivo*

pathogenicity of these cells. In the brains of mice with passive EAE, we discovered, via immunohistofluorescence analysis, that the absolute number of ST14⁺ CD4⁺ T cells was significantly diminished at disease onset in MCAM KO recipient mice, as compared to their WT counterpart (Fig. 5P and Q). In multiple sclerosis, flow cytometry analysis of rapid brain autopsies showed that the presence of ST14⁺ CD4⁺ T lymphocytes is significantly greater in multiple sclerosis lesions than in normal appearing tissues (Fig. 5R). The combination of observations highlighted in this section suggest that ST14 on CD4⁺ T lymphocytes interacts with MCAM on BBB ECs to promote their brain infiltration in autoimmune neuroinflammation.

Discussion

Multiple sclerosis and its lesions develop as a consequence of CNS infiltration by pathogenic immune cells. This neuroinflammatory process is often investigated while almost exclusively focusing on the migrating immune cell. In this study, we instead adopted an approach that began with the receiving BBB ECs. We hereby report that MCAM on brain ECs is tightly associated with autoimmune neuroinflammation and demonstrate that it promotes disease development by specifically recruiting pathogenic CD4⁺ T lymphocytes from circulation. Our approach also pinpointed ST14 as a ligand of MCAM, expressed on inflammatory CD4⁺ T lymphocytes and enriched on migrating CD4⁺ T lymphocytes *in vitro*, in EAE brain and in multiple sclerosis lesions.

In multiple sclerosis, it is widely believed that immune cells infiltrate the CNS parenchyma mainly through post-capillary venules.^{41,42} To our knowledge, this dogma was mostly based on a study of peripheral immune cell trafficking in cats in the 1980s and more recent circumstantial evidence^{41–43}. At the single-cell RNA level, our data support this notion. We first showed that *Mcam*⁺ ECs in EAE are associated with a marked inflammatory profile. At a higher single-cell resolution, we identified a subset of brain capillary-to-venous ECs upregulated in EAE and which reacts to neuroinflammation by upregulating cell adhesion pathways. In parallel, we also detected *Mcam* expression along the arterial arm of the vascular tree in the brains of both naïve and EAE animals. Whether MCAM on capillary-to-arterial brain ECs is involved in homeostatic or pathogenic functions is a question worth investigating in the future.

At the pathological level, multiple sclerosis is characterized by the presence of multifocal CNS lesions. However, the biological factors dictating the anatomical dispersion of these lesions remain unclear.² Our study provides some clues regarding this conundrum. In EAE, our single-cell analysis revealed that *Mcam* mRNA is detected in <5% of brain ECs and our mMRI imaging showed seemingly random scattering of MCAM signal throughout the brain. In multiple sclerosis, the presence of MCAM protein on cerebral microvessels was highest in lesions with immune cell presence and in areas adjacent to them. The combination of these findings suggests that CNS microvessels express distinct patterns of cell trafficking molecules, and are thus responsible for recruiting circulating leucocytes and shaping lesion distribution. It was also recently shown by two-photon microscopy that CNS vessels tend to express either ICAM-1 or VCAM-1, and rarely both at the same time.⁴⁴ A study focused on thoroughly characterizing CNS blood vessels at the singular and regional levels would certainly be a breakthrough towards solving this riddle.

In this study, we also demonstrate that MCAM on brain ECs is generally not present on the luminal side of brain ECs under physiological condition and during general inflammation, but that it is at onset of autoimmune neuroinflammation. This was

achieved by adopting a previously published and thoroughly validated mMRI framework.^{25,26} Fournier *et al.*²⁶ reported that measuring the luminal presence of the cell trafficking molecule P-selectin on spinal cord ECs, but not brain ECs, can predict EAE disease development, relapses and remissions. Our observations do not only complement this study by showing that MCAM is perhaps a cerebral cell trafficking molecule while P-selectin is strictly a spinal cord one, but they also propose MCAM as a potential mMRI prognostic alternative to P-selectin.

The data herein presented also has therapeutic implications. The approved therapy natalizumab has already showcased how pharmaceutically blocking a cell trafficking molecule, and hence leucocyte migration into the CNS, is an effective approach to treat multiple sclerosis. The clinical efficacy of natalizumab, however, was overshadowed by adverse CNS safety events because of the expression of its molecular target, VLA-4, on almost all circulating immune cells.^{45–47} Unlike VLA-4, MCAM expression was previously shown to be restricted to pathogenic T lymphocytes and used by them to infiltrate the CNS during autoimmune neuroinflammation.^{12,13,19} On VLA-4 blockade, lymphocytes were found to even use MCAM as an alternative cell trafficking molecule to invade the CNS.⁴⁸ MCAM was hence proposed as a promising therapeutic target for multiple sclerosis. This paper strongly supports this hypothesis. The luminal presence of MCAM on the cerebrovasculature exclusively during autoimmune neuroinflammation demonstrates that its antibody-mediated targeting is potentially safe for the CNS. The role of MCAM on BBB ECs in recruiting pathogenic but not broadly activated CD4⁺ T lymphocytes suggests that its therapeutic blocking will likely be specific to disease-inducing cells. Altogether, the series of studies on MCAM, including ours, establish it as a promising therapeutic target for next-generation anti-cell trafficking multiple sclerosis therapies.

Last, we hereby showed that the serine protease ST14, a known ligand to endothelial MCAM⁴⁹ is expressed on a subset of CD4⁺ T lymphocytes, which in turn accumulate in both EAE brain and multiple sclerosis lesions. The trafficking of ST14⁺ CD4⁺ T lymphocytes across BBB ECs was shown to be significantly reduced when MCAM on human BBB ECs was selectively blocked *in vitro* and in its absence on mouse BBB ECs in EAE. Interestingly, the physical binding of endothelial MCAM to ST14 was demonstrated to occur specifically through ST14's CUB domains, thereby leaving its protease domain free.⁴⁹ In other studies, the catalytic activity of ST14 was reported to regulate the epithelial barrier in the gut and promote cancer invasiveness by degrading extracellular matrix.^{50,51} Therefore, in addition to promoting the initial contact of pathogenic leucocytes with the BBB ECs, ST14 could well be involved in their penetration deep within the CNS during autoimmune neuroinflammation.

In conclusion, this study showcased MCAM⁺ brain blood vessels as important trafficking hubs for CD4⁺ T lymphocytes during autoimmune neuroinflammation. We demonstrated that blocking MCAM on BBB ECs impaired CNS infiltration and alleviated disease, and identified the MCAM-ST14 pathway as potentially pathogenic in multiple sclerosis. By building on the reported findings, future research could lead to the development of a novel and promising class of anti-CNS leucocyte infiltration therapeutics for treating multiple sclerosis.

Acknowledgements

We are grateful to the Small Animal Imaging Labs at the Research Institute of the McGill University Health Centre (RI-MUHC) and its

staff, particularly Mathieu Simard and Antonio Aliaga, for their help in conducting the mMRI experiments. We also thank the CRCHUM's animal facility led by H el ene H. H eon, the transgenic platform led by Mitra Cowan, the imaging platform led by Aur elie A. Cleret-Buhot, the flow cytometry platform led by Dominique D. Gauchat, and their entire staff, particularly Alice Michallet Roy, for their expertise and enthusiastic support during the completion of this specific project.

Funding

This study was supported by funding from the Multiple Sclerosis Society of Canada (MSSC). During the completion of this study, M.C. and C.G. held scholarships from the MSSC; S.Z., M.-A.L., B.Z. and E.P. were supported by a joint Fonds de Recherche du Qu ebec - Sant e (FRQS)-MSSC fellowship; A.P.F. and K.T. held scholarships from the Canadian Institutes of Health Research (CIHR) and F.T. was supported by a fellowship from Roche. C.L. holds a salary award from the FRQS. A.P. holds the T1 Canada Research Chair in Multiple Sclerosis and is funded by the CIHR, the MSSC, the International Progressive MS Alliance and the Canadian Foundation for Innovation.

Competing interests

R.C., C.L., N.A. and A.P. are inventors on patents and patent applications related to MCAM modulation and uses thereof (CA2676962C, AU2009212789B2, US8293468B2 and US9017682B2). A.P. is an inventor on patents and patent applications related to DICAM-specific antibodies and uses thereof (US10428144B2, WO2016095046A1, EP3233919B1 and CA2971364A1). E.P. is currently an employee of Immunic AG and owns stock options of the parent company of Immunic AG.

Supplementary material

Supplementary material is available at *Brain* online.

References

- Kuhlmann T, Ludwin S, Prat A, Antel J, Br uck W, Lassmann H. An updated histological classification system for multiple sclerosis lesions. *Acta Neuropathol.* 2017;133:13-24.
- Reich DS, Lucchinetti CF, Calabresi PA. Multiple sclerosis. *N Engl J Med.* 2018;378:169-180.
- Daneman R, Prat A. The blood-brain barrier. *Cold Spring Harb Perspect Biol.* 2015;7:a020412.
- Cramer SP, Simonsen H, Frederiksen JL, Rostrup E, Larsson HBW. Abnormal blood-brain barrier permeability in normal appearing white matter in multiple sclerosis investigated by MRI. *Neuroimage Clin.* 2014;4:182-189.
- Miller DH, Leary SM. Primary-progressive multiple sclerosis. *Lancet Neurol.* 2007;6:903-912.
- Arnold DL, Li D, Hohol M, et al. Evolving role of MRI in optimizing the treatment of multiple sclerosis: Canadian consensus recommendations. *Mult Scler J Exp Transl Clin.* 2015;1:2055217315589775.
- Absinta M, Sati P, Reich DS. Advanced MRI and staging of multiple sclerosis lesions. *Nat Rev Neurol.* 2016;12:358-368.
- Lassmann H. Pathogenic mechanisms associated with different clinical courses of multiple sclerosis. *Front Immunol.* 2019;9:3116.
- Alvarez JI, Saint-Laurent O, Godschalk A, et al. Focal disturbances in the blood-brain barrier are associated with formation of neuroinflammatory lesions. *Neurobiol Dis.* 2015;74:14-24.
- Charabati M, Rabanel J-M, Ramassamy C, Prat A. Overcoming the brain barriers: From immune cells to nanoparticles. *Trends Pharmacol Sci.* 2020;41:42-54.
- Larochelle C, Alvarez JI, Prat A. How do immune cells overcome the blood-brain barrier in multiple sclerosis? *FEBS Lett.* 2011;585:3770-3780.
- Larochelle C, Cayrol R, Kebir H, et al. Melanoma cell adhesion molecule identifies encephalitogenic T lymphocytes and promotes their recruitment to the central nervous system. *Brain.* 2012;135:2906-2924.
- Breuer J, Korpos E, Hannocks M-J, et al. Blockade of MCAM/CD146 impedes CNS infiltration of T cells over the choroid plexus. *J Neuroinflammation.* 2018;15:236.
- Cayrol R, Wosik K, Berard JL, et al. Activated leukocyte cell adhesion molecule promotes leukocyte trafficking into the central nervous system. *Nat Immunol.* 2008;9:137-145.
- L ecuyer M-A, Saint-Laurent O, Bourbonni ere L, et al. Dual role of ALCAM in neuroinflammation and blood-brain barrier homeostasis. *Proc Natl Acad Sci USA.* 2017;114:E524-E533.
- Charabati M, Grasmuck C, Ghannam S, et al. DICAM Promotes TH17 lymphocyte trafficking across the blood-brain barrier during autoimmune neuroinflammation. *Sci Transl Med.* 2022;14:eabj0473.
- Wang Z, Yan X. CD146, A multi-functional molecule beyond adhesion. *Cancer Lett.* 2013;330:150-162.
- Wang Z, Xu Q, Zhang N, Du X, Xu G, Yan X. CD146, from a melanoma cell adhesion molecule to a signaling receptor. *Signal Transduct Target Ther.* 2020;5:148.
- Larochelle C, L ecuyer M-A, Alvarez JI, et al. Melanoma cell adhesion molecule-positive CD8 T lymphocytes mediate central nervous system inflammation. *Ann Neurol.* 2015;78:39-53.
- Munji RN, Soung AL, Weiner GA, et al. Profiling the mouse brain endothelial transcriptome in health and disease models reveals a core blood-brain barrier dysfunction module. *Nat Neurosci.* 2019;22:1892-1902.
- Fournier AP, Tastet O, Charabati M, et al. Single-cell transcriptomics identifies brain endothelium inflammatory networks in experimental autoimmune encephalomyelitis. *Neurol Neuroimmunol Neuroinflamm.* 2022;10(1):e200046.
- Thompson AJ, Banwell BL, Barkhof F, et al. Diagnosis of multiple sclerosis: 2017 revisions of the McDonald criteria. *Lancet Neurol.* 2018;17:162-173.
- Dhaeze T, Tremblay L, Lachance C, et al. CD70 Defines a subset of proinflammatory and CNS-pathogenic TH1/TH17 lymphocytes and is overexpressed in multiple sclerosis. *Cell Mol Immunol.* 2019;16:652-665.
- Kebir H, Ifergan I, Alvarez JI, et al. Preferential recruitment of interferon-gamma-expressing TH17 cells in multiple sclerosis. *Ann Neurol.* 2009;66:390-402.
- Montagne A, Gauberti M, Macrez R, et al. Ultra-sensitive molecular MRI of cerebrovascular cell activation enables early detection of chronic central nervous system disorders. *Neuroimage.* 2012;63:760-770.
- Fournier AP, Quenault A, Martinez de Lizarrondo S, et al. Prediction of disease activity in models of multiple sclerosis by molecular magnetic resonance imaging of P-selectin. *Proc Natl Acad Sci USA.* 2017;114:6116-6121.
- Ifergan I, Kebir H, Alvarez JI, et al. Central nervous system recruitment of effector memory CD8+ T lymphocytes during

- neuroinflammation is dependent on $\alpha 4$ integrin. *Brain*. 2011;134:3560-3577.
28. Prat A, Biernacki K, Becher B, Antel JP. B7 expression and antigen presentation by human brain endothelial cells: Requirement for proinflammatory cytokines. *J Neuropathol Exp Neurol*. 2000;59:129-136.
 29. Biernacki K, Prat A, Blain M, Antel JP. Regulation of Th1 and Th2 lymphocyte migration by human adult brain endothelial cells. *J Neuropathol Exp Neurol*. 2001;60:1127-1136.
 30. Ifergan I, Wosik K, Cayrol R, et al. Statins reduce human blood-brain barrier permeability and restrict leukocyte migration: Relevance to multiple sclerosis. *Ann Neurol*. 2006;60:45-55.
 31. Michel L, Grasmuck C, Charabati M, et al. Activated leukocyte cell adhesion molecule regulates B lymphocyte migration across central nervous system barriers. *Sci Transl Med*. 2019;11:eaaw0475.
 32. Broux B, Zandee S, Gowing E, et al. Interleukin-26, preferentially produced by TH17 lymphocytes, regulates CNS barrier function. *Neurol Neuroimmunol Neuroinflamm*. 2020;7:e870.
 33. Podjaski C, Alvarez JI, Bourbonnière L, et al. Netrin 1 regulates blood-brain barrier function and neuroinflammation. *Brain*. 2015;138:1598-1612.
 34. Larochelle C, Metz I, Lécuyer M-A, et al. Immunological and pathological characterization of fatal rebound MS activity following natalizumab withdrawal. *Mult Scler*. 2017;23:72-81.
 35. Kebir H, Kreymborg K, Ifergan I, et al. Human TH17 lymphocytes promote blood-brain barrier disruption and central nervous system inflammation. *Nat Med*. 2007;13:1173-1175.
 36. Vanlandewijck M, He L, Mäe MA, et al. A molecular atlas of cell types and zonation in the brain vasculature. *Nature*. 2018;554:475-480.
 37. Bardin N, Anfosso F, Massé JM, et al. Identification of CD146 as a component of the endothelial junction involved in the control of cell-cell cohesion. *Blood*. 2001;98:3677-3684.
 38. Muller WA, Ratti CM, McDonnell SL, Cohn ZA. A human endothelial cell-restricted, externally disposed plasmalemmal protein enriched in intercellular junctions. *J Exp Med*. 1989;170:399-414.
 39. Lertkiatmongkol P, Liao D, Mei H, Hu Y, Newman PJ. Endothelial functions of platelet/endothelial cell adhesion molecule-1 (CD31). *Curr Opin Hematol*. 2016;23:253-259.
 40. Dagur PK, Biancotto A, Wei L, et al. MCAM-expressing CD4(+) T cells in peripheral blood secrete IL-17A and are significantly elevated in inflammatory autoimmune diseases. *J Autoimmun*. 2011;37:319-327.
 41. Nishihara H, Engelhardt B. Brain barriers and multiple sclerosis: Novel treatment approaches from a brain barriers perspective. *Handb Exp Pharmacol*. 2022;273:295-329.
 42. Engelhardt B, Ransohoff RM. Capture, crawl, cross: The T cell code to breach the blood-brain barriers. *Trends Immunol*. 2012;33:579-589.
 43. House SD, Lipowsky HH. Leukocyte-endothelium adhesion: Microhemodynamics in mesentery of the cat. *Microvasc Res*. 1987;34:363-379.
 44. Mastorakos P, Mihelson N, Luby M, et al. Temporally distinct myeloid cell responses mediate damage and repair after cerebrovascular injury. *Nat Neurosci*. 2021;24:245-258.
 45. Bloomgren G, Richman S, Hotermans C, et al. Risk of natalizumab-associated progressive multifocal leukoencephalopathy. *N Engl J Med*. 2012;366:1870-1880.
 46. O'Connor P, Goodman A, Kappos L, et al. Long-term safety and effectiveness of natalizumab redosing and treatment in the STRATA MS study. *Neurology*. 2014;83:78-86.
 47. Stüve O, Marra CM, Jerome KR, et al. Immune surveillance in multiple sclerosis patients treated with natalizumab. *Ann Neurol*. 2006;59:743-747.
 48. Schneider-Hohendorf T, Rossaint J, Mohan H, et al. VLA-4 blockade promotes differential routes into human CNS involving PSGL-1 rolling of T cells and MCAM-adhesion of TH17 cells. *J Exp Med*. 2014;211:1833-1846.
 49. Tung H-H, Lee S-L. Physical binding of endothelial MCAM and neural transmembrane protease matriptase-novel cell adhesion in neural stem cell vascular niche. *Sci Rep*. 2017;7:4946.
 50. Uhland K. Matriptase and its putative role in cancer. *Cell Mol Life Sci*. 2006;63:2968-2978.
 51. Tanabe LM, List K. The role of type II transmembrane serine protease-mediated signaling in cancer. *FEBS J*. 2017;284:1421-1436.